

Detailed band structure for 3C-, 2H-, 4H-, 6H-SiC, and Si around the fundamental band gap

C. Persson

Department of Physics and Measurement Technology, Linköping University, S-581 83 Linköping, Sweden

U. Lindefelt

*Department of Physics and Measurement Technology, Linköping University, S-581 83 Linköping, Sweden
and ABB Corporate Research, S-721 78 Västerås, Sweden*

(Received 9 July 1996)

Electron and hole effective masses for the polytypes 3C-, 2H-, 4H-, and 6H-SiC have been calculated within the framework of the local density approximation including spin-orbit interaction. To establish the accuracy of the approximations, effective masses for both electrons and holes in Si have also been calculated. It is found that the agreement with well-established experimental values is excellent both for Si and SiC. The valence bands have been parametrized in terms of $\mathbf{k}\cdot\mathbf{p}$ parameters. [S0163-1829(96)08739-5]

Because of the rather recent progress in crystal growth^{1,2} the worldwide interest in SiC for electronic device applications is now greater than ever before. In this article we present basic band-structure information for SiC. In particular, we will focus on the detailed shapes of the bands close to the top of the valence bands and the bottom of the conduction bands in the four most common polytypes 3C, 2H, 4H, and 6H of SiC. This information is absolutely essential for describing and understanding electron and hole dynamics in these polytypes.

The band-structure method used is the full-potential linearized augmented-plane-wave method³ within the density-functional theory and the local-density approximation (LDA).⁴ A program⁵ containing the scalar relativistic approximation with the correlation potential of Perdew and Wang⁶ was used. Since LDA is a ground-state theory in which the one-particle energy parameters do not generally correspond to electronic excitations (c.f. the band-gap problem for semiconductors), there is no guarantee that the cur-

vature of the bands in the vicinity of band extrema, as reflected by the effective masses, is well described by the LDA. We have therefore calculated the effective masses and $\mathbf{k}\cdot\mathbf{p}$ parameters also for Si, for which these quantities are considered well known from experiment. As will be seen, our results show that LDA gives the effective masses to within a few percent accuracy. Furthermore, comparison with experimentally determined effective masses for SiC, when available, also shows very good agreement. We therefore expect the calculated curvatures of the energy bands in the vicinity of the band gap to reflect reality very well.

The calculated LDA band gaps and electron effective masses are shown in Table I. (The labeling of symmetry points and symmetry lines in the relevant cubic and hexagonal Brillouin zones (BZ's) is the same as in Ref. 11.) The errors in band-gap values are well known, whereas the calculated effective masses agree with experimental values, when available, to an excellent precision. Almost identical results have been obtained for the three hexagonal polytypes

TABLE I. Calculated and measured values of band gap, electron effective masses (in units of the free electron mass), and positions of the energy minima of the lowest conduction band in the BZ. The experimental band gaps for the SiC polytypes quoted here are the exciton band gaps at $T=4$ K, which are smaller than the usual band gaps by the exciton binding energy, which probably is in the range 20–30 meV. All experimental band gaps are from Ref. 7. The subscripts on the masses for the SiC polytypes indicate which directions in the BZ the mass components refer to. The experimental electron effective masses for Si, 3C-SiC, 4H-, and 6H-SiC are from Refs. 7, 8, 9, and 10, respectively.

Electrons	Si	3C-SiC	2H-SiC	4H-SiC	6H-SiC
E_g (eV, calc)	0.44	1.30	2.11	2.17	1.97
E_g (eV, expt)	1.17	>2.39	>3.33	>3.26	>3.02
Min. (calc)	Γ -X(Δ)	X	K	M	M-L (U)
Masses	$m_1=0.95$	$m_{XU}=0.23$	$m_{K\Gamma}=0.43$	$m_{M\Gamma}=0.57$	$m_{\parallel M\Gamma}=0.75$
(calc)	$m_t=0.19$	$m_{XW}=0.23$	$m_{KM}=0.43$	$m_{MK}=0.28$	$m_{\parallel MK}=0.24$
		$m_{X\Gamma}=0.68$	$m_{KH}=0.26$	$m_{ML}=0.31$	$m_{ML}=1.83$
Masses	$m_1=0.92$	$m_{XU}=0.25$		$m_{M\Gamma}=0.58$	a
(expt)	$m_t=0.19$	$m_{XW}=0.25$		$m_{MK}=0.31$	a
		$m_{X\Gamma}=0.67$		$m_{ML}=0.33$	$m_{ML}=2.0\pm 0.2$

^aExperimentally (see Ref. 10) the geometric average $(m_{\parallel M\Gamma} \cdot m_{\parallel MK})^{1/2}$ equals 0.42, which fully agrees with the theoretical value.

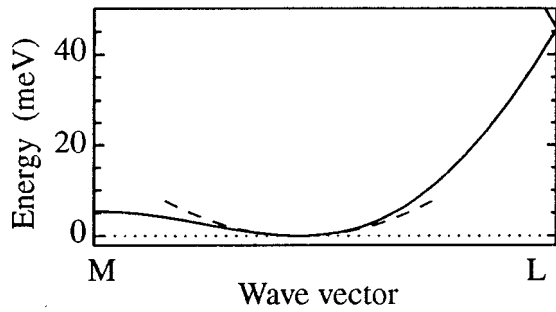


FIG. 1. The shape of the lowest conduction band in $6H$ -SiC along the ML direction. The dashed line represents the parabolic approximation.

by Lambrecht and Segall.¹² Attempts to include quasiparticle corrections, i.e., corrections to LDA, for the electron effective masses in SiC were recently reported.¹³

It should be recognized that, for $6H$ -SiC in particular, the electron effective-mass values given above are valid only in the absolute vicinity of the band minimum. This is illustrated in Fig. 1, which shows that even for a modest band filling due to, for instance, thermal effects or doping, the band curvature is not well represented by the effective-mass values in Table I. At the point M the lowest conduction band has a saddle point only about 5.3 meV above the minimum located at 44.3% of the distance from M to L .

To our knowledge hole effective masses for SiC polytypes have not been measured. A few calculations have recently been performed, however. For instance, Willatzen, Cardona, and Christensen¹⁴ calculated the hole effective masses for $3C$ -SiC, while Käckell, Wenzien, and Bechstedt¹⁵ calculated the hole effective masses for the hexagonal polytypes $2H$ -, $4H$ -, and $6H$ -SiC. In contrast to Willatzen, Cardona, and Christensen, the authors of Ref. 15 did not include spin-orbit interaction, which can lead to totally inaccurate hole masses. To establish to some degree the accuracy of the computational method used here for calculating hole effective masses for SiC, we have again applied the method to Si. The results are presented in the upper part of Table II. As for electrons, the agreement with measured hole masses and valence-band parameters is very good.

In Fig. 2 we illustrate the decisive role played by spin-orbit coupling in determining the hole effective masses. The figure shows constant energy surfaces for energy $E = 1$ meV below each valence-band maximum for the three highest valence bands in the cases of spin-orbit interaction excluded

TABLE II. Spin-orbit splitting, average hole masses (in units of the free electron mass) for heavy hole, light hole, and spin-orbit split-off bands, and valence-band $\mathbf{k} \cdot \mathbf{p}$ parameters A , B , and C [see Eq. (1)] for the cubic polytypes of Si and SiC. For Si both calculated and measured values are given, whereas the values for $3C$ -SiC are calculated. The experimental Si hole masses quoted here are calculated from the experimental values of A , B , and C (Ref. 7).

Holes	Δ_{so} (meV)	m_{hh}	m_{lh}	m_{so}	A	$ B $	$ C $
Si (calc)	50.1	0.43	0.15	0.22	-4.61	0.78	5.17
Si (expt)	44.1	0.46	0.16	0.23	-4.27	0.63	4.93
$3C$ -SiC	14.5	1.01	0.34	0.51	-1.96	0.30	2.27

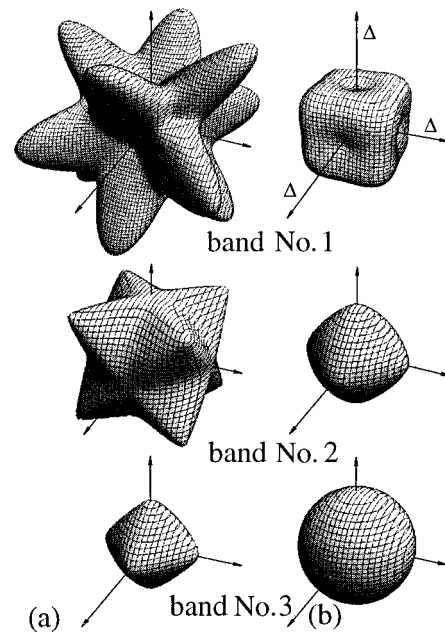


FIG. 2. Constant energy surfaces around Γ for the three highest valence bands in Si without spin-orbit interaction (a) and with spin-orbit interaction included (b). The constant energy $E = 1$ meV below each valence-band maximum.

[Fig. 2(a)] and spin-orbit interaction included [Fig. 2(b)]. It is clear that spin-orbit interaction has totally reshaped the constant energy surfaces for the two highest (degenerate at Γ) valence bands (#1 and #2), and that the third (spin-orbit split-off) band becomes essentially spherical when spin-orbit interaction is included.

Having established the accuracy of the computational scheme for Si, we now go on to describe the results obtained

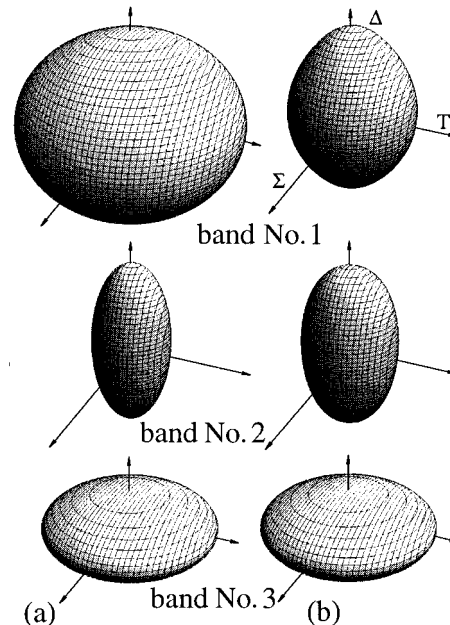


FIG. 3. Constant energy surfaces around Γ for the three highest valence bands in $2H$ -SiC without spin-orbit interaction (a) and with spin-orbit interaction included (b). The constant energy $E = 4$ meV below each valence-band maximum.

TABLE III. Crystal-field splitting Δ_{cf} , spin-orbit splitting Δ_{so} , and dimensionless valence-band parameters a and b [see Eq. (2) in the main text] for three hexagonal polytypes of SiC.

Holes	2H-SiC	4H-SiC	6H-SiC
Δ_{cf} (meV)	161	73	54
Δ_{so} (meV)	8.8	8.6	8.5
a	-4.88	-4.73	-4.82
b	-0.66	-0.67	-0.65

for the SiC polytypes. The shapes of the constant energy surfaces in 3C-SiC at $E=1$ meV below each valence-band maximum are qualitatively very similar to those for Si. The differences essentially lie in the lengths of the ‘‘arms’’ sticking out when spin-orbit interaction is not included. These arms are even longer for 3C-SiC (larger masses) than for Si. For instance, the effective mass along Σ is 15.0 before spin-orbit interaction is included, but is reduced to 1.32 when spin-orbit interaction is taken into account.

The results for the valence-band structures presented above can conveniently be expressed in terms of the equations^{7,16}

$$E_{\text{hh, lh}}(\mathbf{k}) = \frac{\hbar^2 k^2}{2m_0} (A \pm \sqrt{B^2 + sC^2}), \quad (1a)$$

$$s = (k_x^2 k_y^2 + k_y^2 k_z^2 + k_z^2 k_x^2) / k^4,$$

$$E_{\text{so}}(\mathbf{k}) = -\Delta_{\text{so}} + \frac{\hbar^2 k^2}{2m_0} A, \quad (1b)$$

which have their origin in the second-order perturbation approximation in the $\mathbf{k} \cdot \mathbf{p}$ method. In Eq. (1) \mathbf{k} is the crystal wave vector and m_0 is the free electron mass. The calculated spin-orbit splitting Δ_{so} and $\mathbf{k} \cdot \mathbf{p}$ parameters A , B , and C for 3C-SiC and Si are presented in Table II together with the experimental values for Si. The *average* masses for the heavy hole (hh), light hole (lh) and spin-orbit (so) split-off bands in Table II are determined from⁷ $m_{\text{hh, lh}} = -[A \pm (B^2 + C^2/6)^{1/2}]^{-1}$ and $m_{\text{so}} = 1/|A|$. A comparison with Ref. 14 reveals that the two calculations give similar results for 3C-SiC.

It should be noted that spin-orbit interaction only mixes states that are degenerate or nearly degenerate. For instance, we obtain the same hole effective masses whether we include only the three uppermost valence bands or all valence and conduction bands in the spin-orbit matrix. Furthermore, the effects of spin-orbit interaction on the effective masses decreases rapidly as we move away from the Γ point.

In Fig. 3 we show constant energy surfaces for energy $E=4$ meV below each valence-band maximum for one of the hexagonal polytypes, namely, 2H-SiC. For this polytype the effect of spin-orbit interaction is to reduce (increase) the effective mass for the highest (middle) valence band for the directions ΓM ($=\Sigma$) and ΓK ($=T$) in the BZ, whereas the effective mass in the ΓA ($=\Delta$) direction remains the same. The third band is insensitive to the inclusion of spin-orbit interaction. The corresponding results for the 4H and 6H polytypes are qualitatively very similar.

TABLE IV. Dimensionless valence-band parameters c , c' , c'' , d , d' , and d'' [see Eq. (2) in the main text] for three hexagonal polytypes of SiC.

Holes	c	c'	c''	d	d'	d''
2H-SiC	-0.65	0.01	-0.01	-1.73	-0.04	1.02
4H-SiC	-0.64	0.03	-0.03	-1.70	-0.03	1.01
6H-SiC	-0.65	0.04	0.02	-1.73	-0.05	1.07

The expressions corresponding to Eq. (1) but valid for wurtzite structure are given by⁷

$$E_{1,2}(\mathbf{k}) = \pm \frac{\Delta_{\text{so}}}{4} + \frac{\hbar^2}{2m_0} \left[ck_{\parallel}^2 + dk_{\perp}^2 \pm \sqrt{\left(\frac{2m_0}{\hbar^2} \frac{\Delta_{\text{so}}}{4} + c'k_{\parallel}^2 + d'k_{\perp}^2 \right)^2 + (c''k_{\parallel}^2 + d''k_{\perp}^2)^2} \right] \quad (2a)$$

$$E_3(\mathbf{k}) = -\Delta_{\text{cf}} + \frac{\hbar^2}{2m_0} (ak_{\parallel}^2 + bk_{\perp}^2), \quad (2b)$$

where k_{\parallel} and k_{\perp} are the components of the wave vector parallel and orthogonal to the hexagonal c axis, respectively. We have applied these expressions to describe the valence-band structure for all three polytypes 2H-, 4H-, and 6H-SiC. The parameters resulting from this fitting are presented in Tables III and IV. The crystal-field splitting parameter Δ_{cf} is affected only very slightly by spin-orbit interaction. Thus, the splitting Δ_{cf} is still almost entirely an effect of crystal-field interaction.

The shapes of the constant energy surfaces turn out to be very similar for all the hexagonal polytypes discussed here. This is also evident from Tables III and IV. Thus, we conclude that the highest valence-band structures for the three polytypes 2H-, 4H-, and 6H-SiC are very similar, whereas, as we have seen above, the lowest conduction-band structures differ considerably.

According to experimental estimates,¹⁷ Δ_{so} is around 10 meV for 3C- and around 5–7 meV for 6H-SiC, while we find somewhat higher values, namely 14.4 and 8.5 meV, respectively. The calculated value for Δ_{so} was a little too high (14%) also for Si (see Table II). The much smaller values of Δ_{so} for SiC compared to Si are consistent with the mainly C-like valence-band maxima.

Finally, it should be noted that in all the calculations presented here, both for electrons and holes, the effects of spin splitting (which, for instance, can take the top of the valence bands *away* from the Γ point in crystals lacking inversion symmetry, like all SiC polytypes) have been excluded because of their smallness. The band energies $E(\mathbf{k})$ used here are thus averages over the energies for spin-up (+) and spin-down (−) bands: $E(\mathbf{k}) = [E(\mathbf{k})^+ + E(\mathbf{k})^-] / 2$.

This work was supported by the Swedish Board for Industrial and Technical Development (NUTEK) and the Swedish Research Council for Technical Sciences (TFR). We also acknowledge assistance from Dr. C.-O. Almbladh at the Department of Theoretical Physics, University of Lund, Sweden.

- ¹J. A. Powell *et al.*, Appl. Phys. Lett. **56**, 1442 (1990).
- ²O. Kordina *et al.*, Appl. Phys. Lett. **66**, 1373 (1995).
- ³D. Singh, *Planewaves, Pseudopotentials, and the LAPW Method* (Kluwer Academic, Dordrecht, 1994).
- ⁴P. Hohenberg and W. Kohn, Phys. Rev. **136**, B864 (1964); W. Kohn and L. J. Sham, *ibid.* **140**, A1133 (1965); L. Hedin and B. I. Lundqvist, J. Phys. C **4**, 2064 (1971).
- ⁵P. Blaha, K. Schwarz, P. Dufek, and R. Augustyn, WIEN95, Technical University of Vienna 1995, improved and updated Unix version of the original copyrighted WIEN code, which was published by P. Blaha, K. Schwarz, P. Sorantin, and S. B. Trickey, in Comput. Phys. Commun. **59**, 399 (1990).
- ⁶J. P. Perdew and Y. Wang, Phys. Rev. B **45**, 13 244 (1992).
- ⁷*Physics of Group IV Elements and III-V Compounds*, edited by O. Madelung, Landolt-Börnstein, New Series, Group III, Vol. 17, Pt. a (Springer-Verlag, Berlin, 1982).
- ⁸R. Kaplan and R. J. Wagner, Solid State Commun. **55**, 67 (1985).
- ⁹D. Volm, B. K. Meyer, D. M. Hofmann, W. M. Chen, N. T. Son, C. Persson, U. Lindefelt, O. Kordina, E. Sörman, A. O. Konstantinov, B. Monemar, and E. Janzén, Phys. Rev. B **53**, 15 409 (1996).
- ¹⁰N. T. Son *et al.*, Appl. Phys. Lett. **65**, 3209 (1994).
- ¹¹G. F. Koster, in *Solid State Physics*, edited by F. Seitz and D. Turnbull (Academic, New York, 1957), Vol. 5, p. 173.
- ¹²W. R. L. Lambrecht and B. Segall, Phys. Rev. B **52**, R2249 (1995).
- ¹³B. Wenzien *et al.*, Phys. Rev. B **52**, 10 897 (1995).
- ¹⁴M. Willatzen, M. Cardona, and N. E. Christensen, Phys. Rev. B **51**, 13 150 (1995).
- ¹⁵P. Käckell, B. Wenzien, and F. Bechstedt, Phys. Rev. B **50**, 10 761 (1994).
- ¹⁶G. Dresselhaus, A. F. Kip, and C. Kittel, Phys. Rev. **98**, 368 (1955).
- ¹⁷R. G. Humphreys, D. Bimberg, and W. J. Choyke, J. Phys. Soc. Jpn. **49**, Suppl. A, 519 (1980).